Photodegradation of Alternating *p-tert*-Butylstyrenyl– and *exo*-Norbornyl–CO Copolymers Studied by Multiple-Frequency Time-Resolved Electron Paramagnetic Resonance Spectroscopy

Malcolm D. E. Forbes,*,† James C. Barborak,‡ Katerina E. Dukes,† and Shiyamalie R. Ruberu†

Venable and Kenan Laboratories, Department of Chemistry, University of North Carolina at Chapel Hill, Chapel Hill, North Carolina 27599-3290, and Department of Chemistry, University of North Carolina at Greensboro, Greensboro, North Carolina 27412

Received August 5, 1993®

ABSTRACT: The photodegradation of two alternating R–CO copolymers (R = *p-tert*-butylstyrenyl and *exo*-norbornyl) was studied using time-resolved electron paramagnetic resonance (TREPR) spectroscopy at two different frequencies, X-band (9.5 GHz) and Q-band (35.1 GHz), and by product analysis. For the *tert*-butylstyrenyl–CO copolymer the EPR spectra displayed strong chemically induced dynamic spin polarization (CIDEP) expected for triplet-born radical pairs from the Norrish I α-cleavage reaction. Simulation of the spectra allowed unambiguous assignment of the radicals present as early as 200 ns after the laser flash. The ^{13}C-substituted (^{13}CO) *tert*-butylstyrenyl copolymer showed unusual magnetic field effects on its spin polarization patterns and an additional long-range ^{13}C hyperfine interaction in the benzylic fragment. The *exo*-norbornyl–CO copolymer unexpectedly showed weak EPR signals of *endo*-substituted 2-norbornyl radicals from Norrish I α-cleavage, indicating that the polymer is not completely stereoregular. Product analysis suggests that this polymer also undergoes Norrish type II degradation processes, producing 1,4-biradicals, which are unobservable by TREPR. A discussion of the mechanisms of photodegradation for both polymers and a spectroscopic analysis of the samples before and after photolysis are presented.

Introduction

The photochemistry and photophysics of polymers continue to be subjects of intense interest.[1] In particular, photodegradability is a desirable feature for applications in environmental science and in photoresist technology. Many polymers photodegrade via free-radical intermediates, and two of the best techniques for studying such processes are optical absorption[2] and electron paramagnetic resonance (EPR)[3] spectroscopies. The EPR technique has an advantage over optical methods because of its high structural resolution. Most EPR studies of polymers have been carried out using steady-state techniques[4] with phase-sensitive detection. This results in greater sensitivity but limited time resolution. Under steady-state conditions it is often unclear whether the radicals being observed are produced from primary or secondary photochemical processes or if they are the result of the rearrangement of an initially formed radical. Also, if the photolysis/EPR is carried out at low temperatures in order to stabilize the resulting reactive intermediates,[5] it is typical to obtain spectra with very broad lines that present difficulties in assignment and interpretation.[6] Time-resolved EPR spectroscopy (TREPR) is an alternative technique that has to date not been used to study polymer photodegradation. It has several clear advantages over steady-state experiments: (1) a large concentration of radicals can be produced and detected a short time later using a high-intensity pulsed laser, (2) the phenomenon of chemically induced electron spin polarization (CIDEP) can enhance the sensitivity of the experiment, (3) spin polarization patterns allow detailed information on the spin characteristics of the excited-state precursors to be obtained, (4) spin relaxation and/or chemical reaction rates can be obtained on the submicrosecond time scale, and (5) the spectra obtained nearly always represent the initial reactive intermediates and not those from secondary reactions.

Chart 1

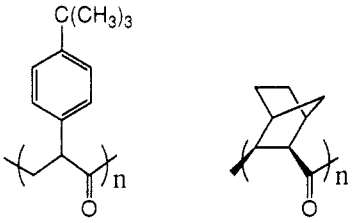

1 **2**

Hartley and Guillet[7] and later Gooden et al.[8] reported mechanistic studies of R–CO copolymer photodegradation, performed on ethylene–CO random copolymers. Quantum yield measurements and product analysis with a particular emphasis on functional group identification showed that both Norrish I α-cleavage and type II elimination processes, along with photooxidation, are important in the degradation of these polymers by near-UV radiation. Hartley and Guillet also reported distinct differences in the photodegradation between the amorphous solid polymer and those dissolved in solution,[7a] showing that conformational flexibility is an important aspect of the destruction of these species. The products from these two fundamental reactions were found to be a sensitive function of polymer structure. In this paper we examine these processes in stereoregular copolymers where the starting structures are very accurately known from mechanistic investigations of their synthesis by catalysis and by characterization studies. Below we report the first real-time EPR detection of monoradicals from the photodegradation of carbonyl-containing polymers, **1** and **2**, whose structures are shown in Chart 1, in solution at room temperature. We will also demonstrate the utility of the multiple-frequency TREPR technique (in tandem with

* Author to whom correspondence should be addressed.
† University of North Carolina at Chapel Hill.
‡ University of North Carolina at Greensboro.
® Abstract published in *Advance ACS Abstracts*, January 15, 1994.

0024-9297/94/2227-1020$04.50/0

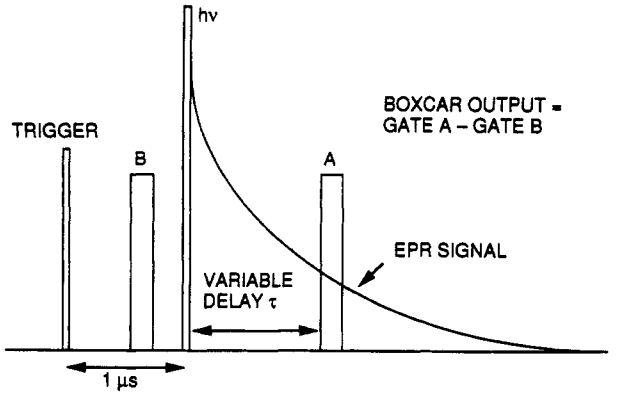

Figure 1. Timing sequence for the time-resolved (direct detection) EPR experiment. See the Experimental Section of the text for details.

product analyses) in identifying primary transient species produced in photochemical reactions of these macromolecules.

Experimental Section

Our time-resolved EPR apparatus has been described previously for both the X-band (9.5 GHz)[9] and Q-band (35.1 GHz)[10] microwave frequencies. X-band experiments were performed on a Jeol USA (Peabody, MA) Inc. JES-RE1X instrument using a Varian TE_{103} optical transmission cavity and flow cells manufactured by NSG Precision Cells, Inc. (Farmingdale, NY). Figure 1 shows the timing sequence for the experiment. The excimer laser (308 nm (XeCl), 17-ns pulse width (fwhm), ≈200 mJ/pulse) excites the sample at a repetition rate of 60 Hz. The boxcar signal averager is used in a two-gate mode, with the first gate opening before the laser flash to measure the dark signal and the second gate sampling the light-induced EPR signal at a fixed delay time τ after the laser flash. The EPR signal at a given delay τ is collected directly from the microwave bridge of the spectrometer and stored digitally as the difference between the two gates while the magnetic field is swept. The gate widths are typically 100 ns, and τ ranged from 0.2 to 3.0 μs (τ is reported as the delay between the peak of the laser flash to the opening of the second boxcar gate). The bridge is equipped with a fast preamplifier which has a 60-ns rise time. The overall time response is limited by the microwave cavity quality factor at about 50 ns at X-band; however, spectra obtained at this delay time are significantly distorted by uncertainty broadening. The samples are recirculated through the cavity to prevent excessive heating. The flat flow cell used at X-band is of 0.75-mm path length, and the rate of flow can be varied from 0.1 to 1 mL s^{-1}. All data shown are individual 2-min scans of the magnetic field unless otherwise indicated. At Q-band, a Varian E110 microwave bridge was used with an E-line 6-in. magnet with tapered pole pieces and a home-built cavity and flow system. The Q-band bridge preamplifier was modified for faster time response (approximately 25-ns rise time). The sensitivity of the Q-band apparatus is approximately a factor of 4 lower than the X-band one; however, the time response is no longer limited by the cavity quality factor but by the laser pulse width and jitter.

Samples of polymer were synthesized according to procedures previously reported.[11] Molecular weight determinations before and after photolysis were performed on a Waters Model 150 CV gel permeation chromatograph against polystyrene standards. GPC analysis of several different samples of polymer 1 before photolysis showed number-average molecular weights (M_n) ranging from 44 000 to 53 000, with dispersities ranging from 1.2 to 1.4. In the case of ^{13}C-substituted polymer 1′, of which only one sample was available, the M_n value was 22 000 with a dispersity of 1.6. For samples of polymer 2, which is synthesized at higher pressures and temperatures than for 1, the M_n values ranged from 3200 to 4900, with dispersities ranging from 1.75 to 2.0. Older samples of 2 (stored for over 1 year) showed significantly lower molecular weights compared to those analyzed immediately after their syntheses. The ^{13}C and ^1H NMR spectra were taken on a Varian XL400 in $CDCl_3$, FTIRs were performed on a Biorad FTS-7 spectrometer, and UV–vis spectra were obtained on a Perkin-Elmer Lambda 6 instrument. TREPR experiments were carried out on solutions of polymer in reagent-grade benzene (0.5 g of polymer per 10 mL of solvent in a typical run). Dry nitrogen gas was bubbled through the samples for 10 min before and during the experiments. In the X-band experiments the laser pulse energy was greater than 50 mJ/pulse, while at Q-band it was estimated to be 3–10 mJ/pulse.

Results and Discussion

A. Photolysis of 1. The chemistry expected during the photolysis of polymer 1 is outlined in Scheme 1. The initial photoexcitation leads to an excited singlet which is expected to efficiently intersystem cross to an excited triplet state. From this state Norrish type I α-cleavage of excited polymer subunits produces a triplet radical pair consisting of a benzylic radical 3 and a primary acyl radical 4. Possible reactions of these species are (1) recombination of the geminate radical pair to reform the alternating copolymer (with scrambling of the initially high stereoregularity), (2) recombination with a like species to form copolymers 5 or 6, or (3) disproportionation to yield either styrene 7 and aldehyde 8 or homobenzylic ketone 9 and ketene 10. Decarbonylation of the primary acyl radical is likely to occur on a slower time scale than recombination or spin relaxation, so this pathway is not considered further here.

The X-band and Q-band time-resolved EPR spectra obtained during the photolysis of polymer 1 are displayed in Figure 2. An asterisk indicates acyl-type radical 4, and all other transitions are assigned to benzylic radical 3. It should be noted that, in contrast to steady-state EPR spectra which are displayed as the first derivative of the absorption curves, these and all subsequent spectra were obtained in direct detection. Transitions above the base line are absorptive, while those below the base line are emissive. This chemically induced electron spin polarization (CIDEP) results from two independent mechanisms. There is a net emission pattern due to the triplet mechanism (TM),[12] and superimposed on this is an emissive/absorptive pattern from the radical pair mechanism (RPM) (low-field lines emissive, high-field lines absorptive).[13] The TM arises from unequal transition probabilities for intersystem crossing from the first excited singlet to the first excited triplet state of the carbonyl chromophore. The RPM polarization arises from nuclear spin-dependent recombination of both geminate and random radical pairs. The presence of these two spin polarization mechanisms leads to an overall emissive spectrum with less intensity in the high-field lines. A representative spectrum from each dataset in Figure 2 is shown for comparison next to a simulated spectrum at each frequency in Figure 3. The values of the g-factors and the hyperfine coupling constants used in the simulations are listed in Table 1. Parameters were obtained by best fit to the simulations for all radicals. The hyperfine values used for the benzylic radical agree well with those obtained from radicals of similar structure.[14] The ratio of TM to RPM polarization and the relative intensity of each radical in both simulations were adjusted to best fit. The excellent agreement between theory and experiment leads us to conclude that Norrish I α-cleavage, as expected, is the dominant photochemical process in this polymer. Product analyses, to be discussed below, confirmed this.

There are some interesting differences between the X- and Q-band spectra shown in Figure 2. The acyl fragments are barely visible at the earliest delay times at X-band and quickly decay by fast spin relaxation to a much weaker

Scheme 1

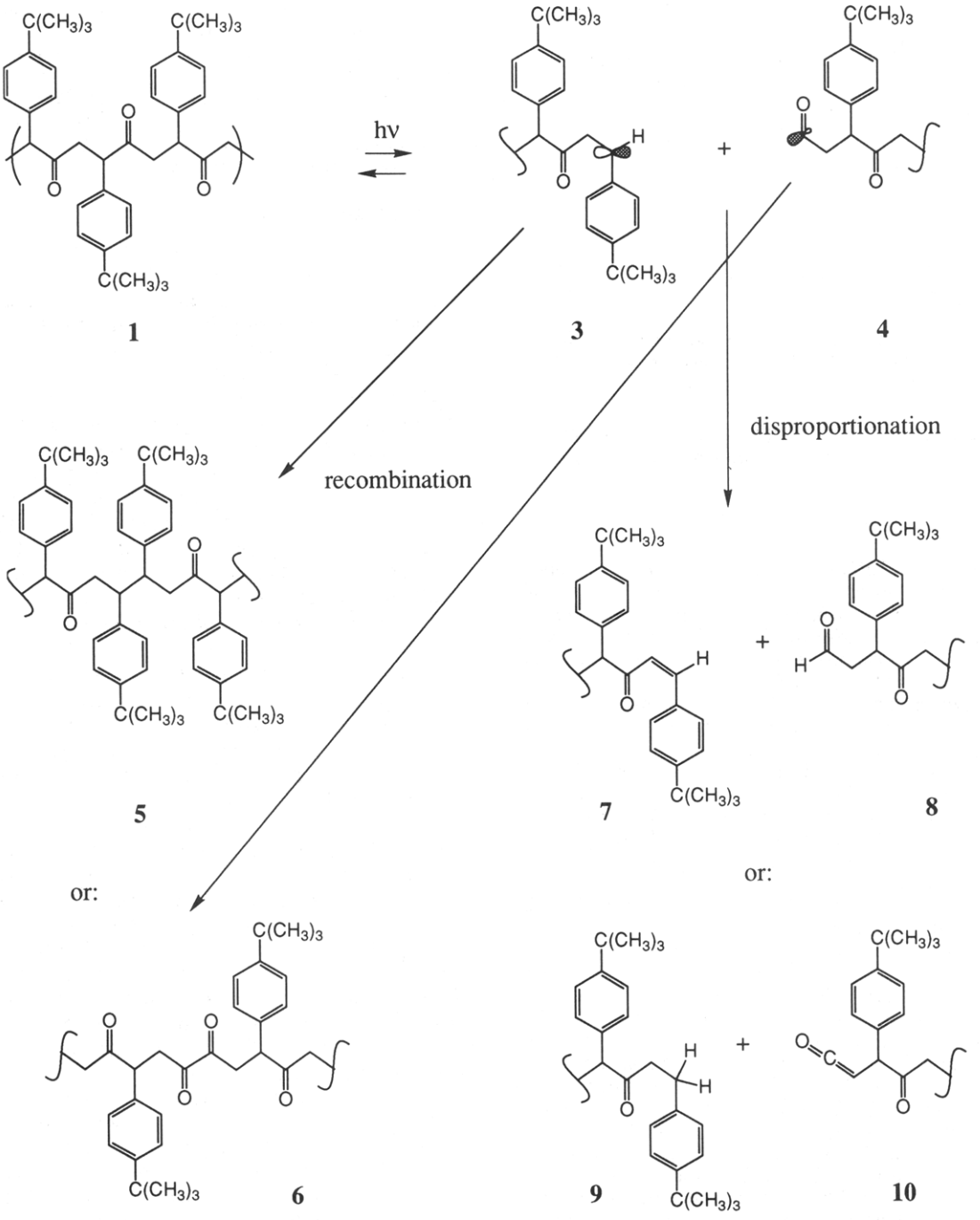

Boltzmann polarization. At Q-band this relaxation is less efficient, and in fact the EPR signal from this radical lasts longer at Q-band than that from the benzylic species. In previous work on monoradicals and biradicals using this apparatus, and by calculation using standard equations,[15] it is possible to show that T_1 can be an order of magnitude longer at Q-band compared to X-band, depending on the solvent viscosity. Also, the *g*-factor (chemical shift) resolution at Q-band is nearly 4 times greater, so there is less overlap of the two signals at the higher microwave frequency. In fact, the two signals are almost completely separated by Q-band (Figure 2b), clearly showing the advantage of performing this experiment at higher frequencies.

Analysis of the products from samples photolyzed over several different time periods showed that the stereoregularity of the polymer is destroyed over approximately 10 min of laser pulses at a 60-Hz repetition rate (~36 000 pulses, 10^{17} photons/pulse). The samples that were photolyzed for long times (>20 min at 60 Hz) became much more crystalline in appearance, as expected for lower molecular weight polymer. Since the freshly synthesized polymer is >90% stereoregular, the ^{1}H NMR spectra show well-resolved peaks for the aromatic chemical shifts in the starting material. These peaks broaden substantially after 10 min of photolysis and significantly more after 20 min. The molecular weight of the polymer decreases much more quickly. The number-average molecular weight dropped from 44 000 to 5000 in just 2 min of photolysis time at the same repetition rate (~7200 laser pulses). The polydispersity approached a limiting value of 1.8 in this time. The NMR technique is not sensitive enough to detect a decrease in stereoregularity during the early part of the photolysis; therefore, GPC measurements are a better indicator of the extent of photodegradation under these conditions. Long-term photolyses (>30 min of laser pulses

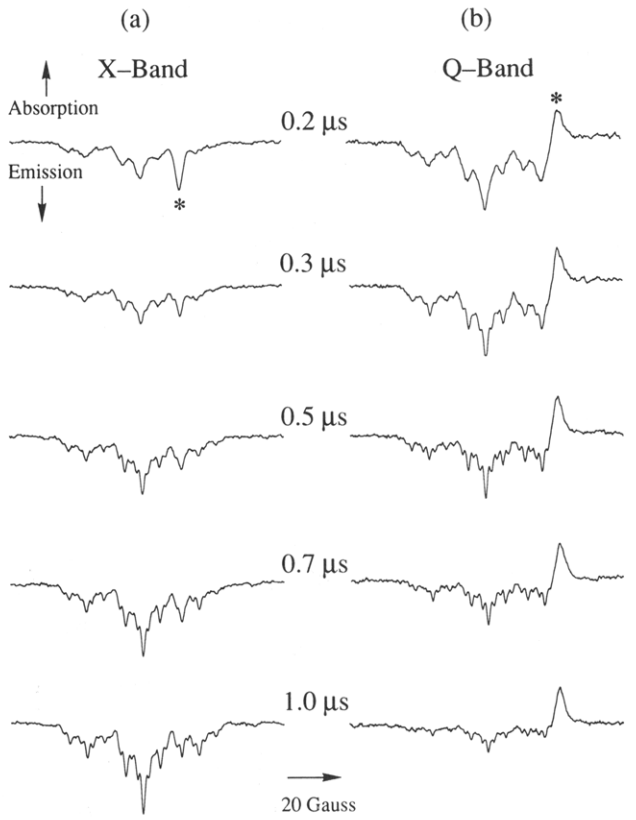

Figure 2. (a) X-band and (b) Q-band TREPR spectra obtained during the photolysis of polymer 1 at room temperature in a benzene solution at the delay times indicated. The concentration of polymer was approximately 5% by weight in both experiments. Here the asterisk indicates the expected position of the acyl radical fragment.

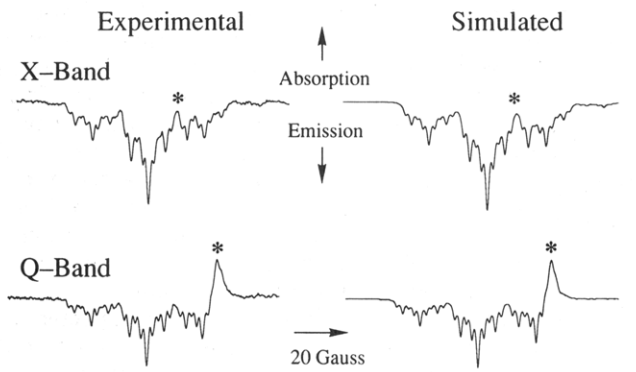

Figure 3. Left: representative spectra from Figure 2, where the asterisk indicates transitions assigned to the acyl radical fragment. All other transitions are assigned to the benzylic fragment. Right: computer simulations of the spectra on the right using the magnetic parameters listed in Table 1. The relative intensity of each radical and the ratio of the triplet mechanism to radical pair mechanism spin polarization were adjusted to best fit in both simulations.

at 60 Hz) showed extremely broad NMR spectra and a limiting value for M_n of about 1500. In photolyses that extended beyond this time, only very minor changes in M_n and M_w were observed. We can suggest the following reason for this limit to the extent of photodegradation: In polymer chains with similar chromophores at regular positions, there is a probability that two excited triplets will annihilate each other to produce an excited singlet, which may then decay radiatively or nonradiatively, or continue to intersystem cross back to the triplet. It is also possible for the excitation to travel along the chain from chromophore to chromophore via energy transfer,[16] mediated by through-bond (and probably also through-solvent) electronic coupling. The probability of triplet–triplet annihilation goes up as the polymer chains become shorter, because of the increased chance of two excitations being closer together.

Structures such as diketone **6** could be identified by UV–vis absorption measurements at 410 nm. This weak band appears halfway between the similar transition in aliphatic (370 nm) and aromatic (440 nm) diketones,[17] as

Table 1. Magnetic Parameters Used in Simulations in Figures 3–5

radical	structure	hyperfine coupling constants (G)	g factor	line width (G)
3	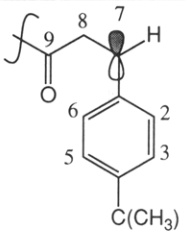	H7 = H8 = 16.3 H2 = H6 = 1.7 H3 = H5 = 4.9	2.0026	2.1
4	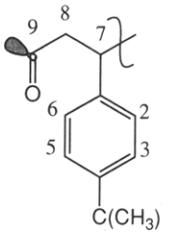	H8 = 1.5	2.0008	4.0
3′	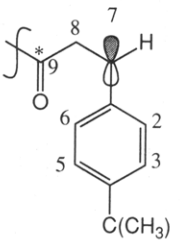	H7 = H8 = 16.3 H2 = H6 = 1.7 H3 = H5 = 4.9 C9 = 9.5	2.0026	2.1
4′	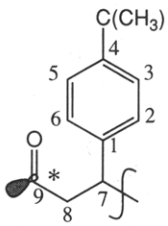	H8 = 1.5 C9 = 129.3	2.0008	4.0
11	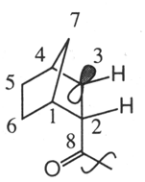	H1 = 6.0 H2 = 37.0 H3 = 20.0 H6 = 8.5 H7 = 2.5	2.0025	1.8
12	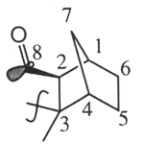	H2 = 1.5	2.0008	4.0

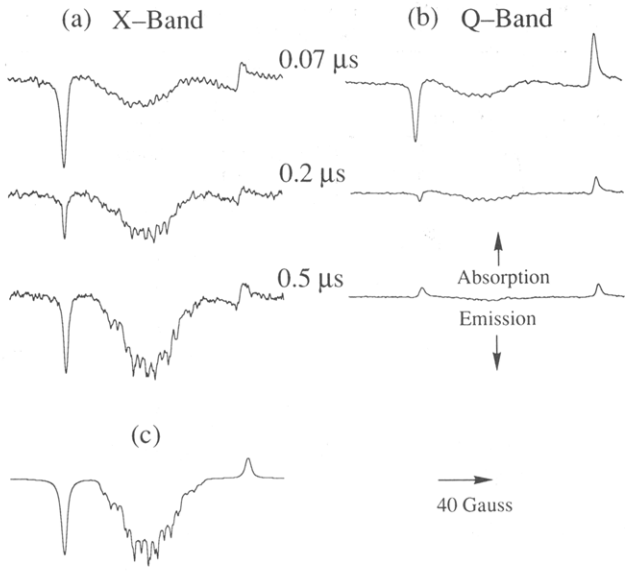

Figure 4. (a) X-band and (b) Q-band TREPR spectra obtained during the photolysis of ^{13}C-containing polymer 1′ (Scheme 2) at room temperature in a benzene solution (≈5% polymer by weight). The signal in the center is assigned to the benzylic radical 3′, while the two outer lines are due to the acyl radical 4′. (c) Simulation of the spectrum in (a) at 0.5 μs, using the parameters listed in Table 1.

expected for a dibenzylic species such as **6**. It is interesting to note that there is a substantial band already present at this wavelength in the starting material. This may be from thermal degradation of the sample, end groups, or connections made in the polymerization reaction by a different mechanism than that previously postulated. After 30 min of photolysis, the absorbance at this wavelength went up by more than a factor of 2 for polymer **1**. IR spectra showed little change after photolysis for all of the samples, presumably because there are still many intact subunits with the carbonyl chromophore present at the limiting molecular weight.

When ^{13}C is substituted (100%) in the carbonyl carbon of polymer **1**, the EPR spectra shown in Figure 4 are obtained and are assigned to radicals **3′** and **4′**, shown in Scheme 2. The acyl fragment exhibits a large hyperfine coupling constant, due to the ^{13}C, of 129.3 G. The RPM theory predicts that the low-field line should be emissive and the high-field line absorptive for a triplet precursor. The benzylic radical, however, should be relatively weak because the polarization obtained by interaction with the low-field acyl radicals is of opposite sign to that obtained by interaction with the high-field acyl radicals. The predicted pattern is seen at early times in the Q-band spectra of this polymer (Figure 4b), but with increasing delay time an unusual intensity change takes place. Both acyl radical peaks become absorptive, while the benzylic radical disappears completely. It is possible that, with the large concentration of radicals produced by each laser flash, at later times we still have enough radicals present that a Boltzmann polarization can be detected. The chemical lifetime of these radicals is expected to be in the range of 10–100 μs, while spin relaxation to a Boltzmann population of the spin states is expected to be on the order of 1–5 μs, consistent with the observed intensity changes in the Q-band spectra in Figure 4. At X-band, the spectra are even more unusual in appearance at all delay times. The benzylic radical grows in intensity with time, and the low-field acyl peak is of the correct phase while the high-field transition appears to be dispersive or it may be exhibiting a splitting due to additional magnetic interaction. At present the origin of this strange line shape is not well understood. They may be caused by the unusually large hyperfine interaction (i.e., a second-order spin-state-mixing effect), the large *g*-factor difference, or by relaxation phenomena caused by the presence of the ^{13}C. This is presently under further investigation. It should also be noted that the benzylic radicals in the X-band spectra in Figure 4 have a different splitting pattern than those in Figures 2 and 3 due to a γ-hyperfine interaction of the ^{13}CO group two carbon atoms away from the benzylic radical center. The coupling constant we obtain by spectral simulation (Figure 4c) of 9.5 G is substantial for a γ-hyperfine interaction and is indicative of either a strong through-space (or solvent) interaction between the carbonyl π-system and the benzylic radical p-orbital or of strong through-bond coupling via σ overlap.

Scheme 2

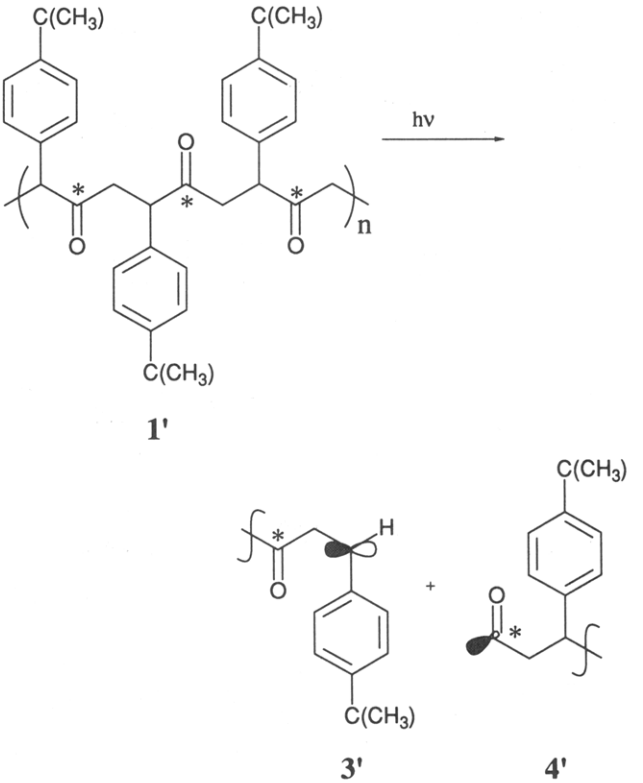

B. Photolysis of 2. This polymer is expected to undergo the photochemical reaction sequence illustrated in Scheme 3. The excitation and intersystem crossing processes described above for **1** are also expected to produce excited triplets in **2**. Because this polymer is more rigid, it may also be expected to fluoresce more readily than polymer **1**, leading to a somewhat lower yield of triplets and therefore slower photodegradation. In polymer **2** the Norrish type I α-cleavage produces secondary norbornyl radical **11** and primary acyl radical **12**. On the basis of previous studies of phenyl–norbornyl ketones by Lewis and co-workers,[18] the dominant reaction is expected to be a type II photoelimination reaction depicted in the top part of the scheme. The polymer is believed to be synthesized with *exo*-stereochemistry exclusively, although we will comment on this further, *vide infra*. The initial 1,5-H-atom abstraction reaction of the triplet would then be from the 7 position of the norbornyl ring system. The resulting 1,4-biradical **13**, if formed in any quantity, can β-eliminate to enol **14**, which then rapidly tautomerizes to its keto form **15**. It is interesting to note that this process does not change the molecular weight of the polymer. Ketone **15** is also photochemically active at the excitation

Scheme 3

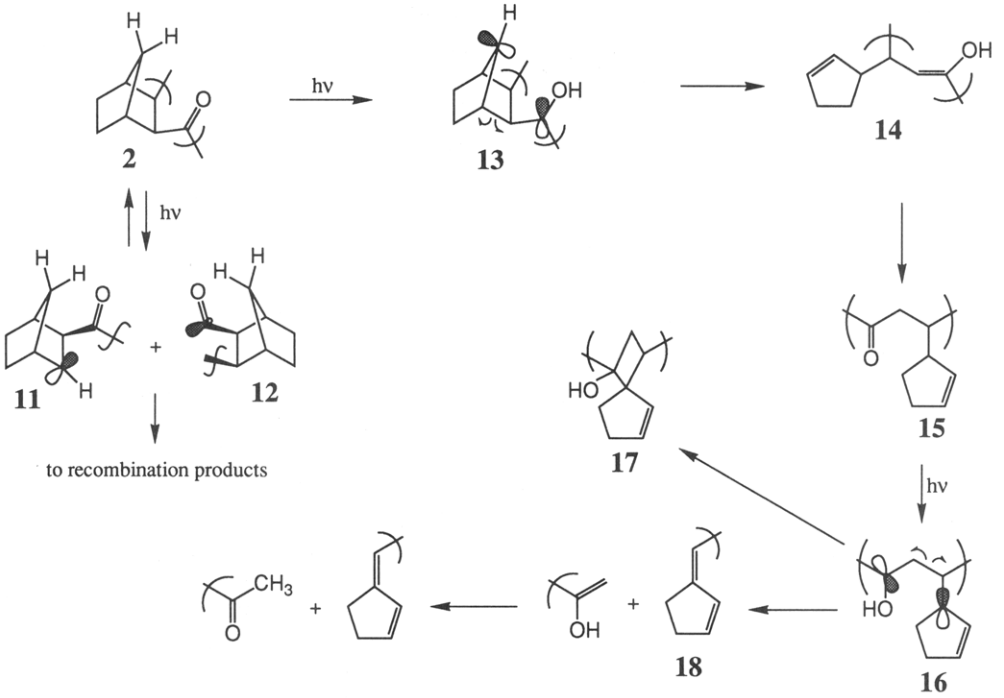

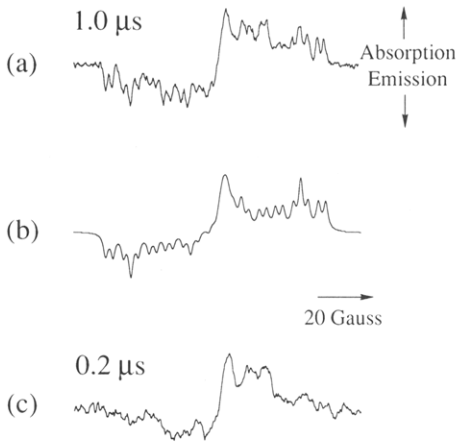

Figure 5. (a) X-band TREPR spectra obtained during the photolysis of polymer **2** in benzene at room temperature. The concentration of polymer was approximately 10% by weight. The experiment was run shortly after the polymer was prepared. (b) Simulation of the spectrum in (a) using the parameters listed in Table 1. (c) Spectrum obtained under experimental conditions similar to those of a except that the sample was several months old, stored in the dark a 0 °C.

wavelength (308 nm) and can be expected to undergo 1,5-H-atom abstraction from the allylic site to produce 1,4-biradical **16**. Localized 1,4-biradicals such as **13** and **16** are as yet undetectable in solution by EPR because the mixing of the singlet and triplet wave functions necessary for strong spin polarization (leading to signal enhancement) is too weak due to the large energy gap between the states.[19] The final reactions of **16** can be ring closure to the spirocyclobutane structure **17** or elimination to products such as diene **18**. The molecular weight of the polymer still does not change if ring closure takes place. Only the final elimination reaction results in a lower molecular weight polymer. From these considerations, it is expected that polymer **2** should reduce in molecular weight over a much slower time scale than polymer **1**.

Figure 5 shows the X-band TREPR spectrum obtained upon photolysis of **2** in benzene at room temperature. Figure 5a shows the spectrum obtained when the sample of polymer has been freshly prepared, while Figure 5c shows the EPR spectrum obtained from photolysis of a sample several months old, stored at 0 °C. Figure 5b shows a simulation which matches peak for peak quite well with those in Figure 5a, although there are some discrepancies in the intensities. We believe that this is due to the presence of other signal carriers such as substituted norbornyl radicals with different stereochemical arrangements and/or radicals from β-elimination of the 2-norbornyl radical system. The spectrum in Figure 5c is very broad, and none of the signals could be accurately assigned except for the acyl radical in the center. The overlap of spectra from several different radicals can cause this, which leads us to conclude that over long time periods this polymer is not thermally stable. No Q-band TREPR signals were obtained for this polymer due to the poor signal-to-noise ratio of the signals and the limited sensitivity of that apparatus. Incorporation of ^{13}CO into this copolymer under high pressure is presently being attempted.

A remarkable feature of the simulation in Figure 5b is the fact that it fits exclusively an *endo*-substituted 2-norbornyl radical and not an *exo*-substituted one. The difference in hyperfine coupling at position 3 between *exo*- and *endo*-substituents is at least 10 G in all of the examples of substituted 2-norbornyl radicals we could find in the literature,[20] a number well outside the tolerance of our simulations (approximately 0.5 G for each hyperfine coupling constant). This means that the predominant photoreaction is α-cleavage from sites along the polymer chain that lead to *endo*-substituted radicals. This can only occur if the polymer is not completely stereoregular; i.e., there are "defects" in the polymer chain where this unexpected photochemistry takes place. This fact was confirmed by noticing that in the ^{13}C NMR of this polymer there are satellites beside the transitions assigned to the ring carbons at the point of attachment to the CO groups. It is, however, troubling that the α-cleavage reaction from the higher concentration *exo–syn* linkages does not appear to be the dominant reaction. There is strong evidence based on studies of model systems in several different

laboratories that the *exo–syn* geometry is preferred in the synthetic pathway.[21] It may be that, in this geometry, the carbonyl groups are strongly coupled, leading to even greater triplet stability or rapid energy migration as discussed above for the polymer 1. Calculations to support this hypothesis are presently underway. There is also the possibility that the excitation coefficient at this wavelength (308 nm) is significantly higher for an *anti*-linkage vs a *syn*-linkage, leading to a higher concentration of radicals by selective excitation of these sites. Again, we are undertaking calculations and experiments to confirm this using model compounds whose structures are accurately known. Based on our starting and ending molecular weights and assuming that cleavage occurs exclusively from the *anti*-moieties, the maximum number of *anti*-links possible in the polymer chains is about 10%, or roughly 3 "defect" sites per polymer chain.

Analysis of the products from the photolysis of polymer 2 by ^{1}H NMR showed the slow growth of vinyl resonances at 5.6 ppm, indicating that some elimination had taken place. Resonances typical of spirocyclobutanes 17 or dienes 18 as shown in Scheme 3 were not observed, even after 1 h of laser pulses. If such dienes were present even in small concentrations, a significant increase in the triplet quenching rates could result. This is another possible explanation for the limiting molecular weight reached at long photolysis times for polymer 2. The change in molecular weight over photolysis time was very slow compared to 1, as predicted above. To go from 4000 to 1500 number-average molecular weight took 30 min to photolysis at 60 Hz (over 10^5 laser pulses). Previously reported product analyses and quenching studies of model compounds *exo*- and *endo*-2-benzoylnorbornane (2-norbornyl phenyl ketone)[18] showed that the *exo*-isomer had a much longer triplet lifetime (almost 3 orders of magnitude) because of slow γ-hydrogen abstraction rates due to conformational constraints. Since the majority of our linkages are believed to be *exo*, this may be why photoelimination products are produced in such small quantities.

Conclusions

We have demonstrated that the time-resolved EPR technique can be a useful tool in the analysis of photodegradation mechanisms of polymers. In tandem with product analyses and through comparisons of the behavior of different polymers, a variety of photochemical processes can be directly observed or inferred from the data. It is interesting that the EPR experiment can actually be used in this case to distinguish between *exo*- and *endo*-stereoisomeric linkages in polymer 2. Polymer 1 photodegrades quickly, while 2 appears to be much more robust photochemically but less stable thermally. These results may be of utility in selectively incorporating photodegradability (or lack of it) into macromolecular structures. Further TREPR and transient optical absorption studies of these and other polymers with very well-defined structures are presently in progress in our laboratories.

Acknowledgment. The authors thank M. S. Brookhart for helpful discussions, G. R. Schulz for experimental assistance, and M. O. Hunt for obtaining the GPC traces. This work was supported by the National Science Foundation through Grant CHE-9200917 and through the NSF National Young Investigator Award Program (to M.D.E.F.; Grant No. CHE-9357108).

References and Notes

(1) (a) Guillet, J. *Polymer Photophysics and Photochemistry*; Cambridge University Press: Cambridge, U.K., 1985. (b) *New Trends in the Photochemistry of Polymers*; Allen, N. S., Rabek, J. F., Eds.; Elsevier: New York, 1985. (c) *Photophysics of Polymers*; Hoyle, C. E., Torkelson, J. M., Eds.; ACS Symposium Series 358; American Chemical Society: Washington, DC, 1987.
(2) Hrdlovic, P.; Scaiano, J. C.; Lukac, I.; Guillet, J. E. *Macromolecules* **1986**, *19*, 1637.
(3) (a) Ranby, B.; Rabek, J. F. *Photodegradation, Photo-oxidation and Photostabilisation of Polymers*; Wiley: London, 1975; Chapter 2. (b) Hill, D. J. T.; O'Donnell, J. H.; Pomery, J. In *Electron Spin Resonance Volume 13A*; Symons, M. C. R., Ed.; Royal Society of Chemistry: Cambridge, U.K., 1992; Chapter 6.
(4) (a) Michel, R. E.; Chapman, F. W.; Mao, T. J. *J. Chem. Phys.* **1966**, *45*, 4604. (b) Gerlock, J. L.; Van Oene, H.; Bauer, D. R. *Eur. Polym. J.* **1983**, *19*, 11. (c) Torikai, A.; Nishiyama, M.; Fueki, K. *Polym. Photochem.* **1984**, *4*, 281. (d) Torikai, A.; Fueki, K. *Polym. Photochem.* **1982**, *2*, 297.
(5) (a) Beachell, H. C.; Chang, I. L. *J. Polym. Sci., Part A* **1972**, *10*, 503. (b) Kubota, H.; Takahashi, K.; Ogiwara, Y. *Polym. Degrad. Stab.* **1988**, *24*, 201. (c) Hon, D. N.-S. *J. Appl. Polym. Sci.* **1979**, *23*, 3591.
(6) Reference 3a, p 60.
(7) (a) Hartley, G. H.; Guillet, J. E. *Macromolecules* **1968**, *1*, 165. (b) Hartley, G. H.; Guillet, J. E. *Macromolecules* **1968**, *1*, 413.
(8) Gooden, R.; Hellman, M. Y.; Hutton, R. S.; Winslow, F. H. *Macromolecules* **1983**, *17*, 2830.
(9) Forbes, M. D. E.; Peterson, J.; Breivogel, C. S. *Rev. Sci. Instrum.* **1991**, *62*, 2662.
(10) Forbes, M. D. E. *Rev. Sci. Instrum.* **1993**, *64*, 397.
(11) Brookhart, M. S.; Rix, F. C.; DeSimone, J. M.; Barborak, J. C. *J. Am. Chem. Soc.* **1992**, *114*, 5894.
(12) (a) *Spin Polarization and Magnetic Effects in Radical Reactions*; Molin, Yu. N., Ed.; Elsevier: New York, 1984; p 224. (b) Atkins, P. W.; Evans, G. T. *Chem. Phys. Lett.* **1974**, *25*, 108. (c) Wong, S. K.; Hutchinson, D. A.; Wan, J. K. S. *J. Chem. Phys.* **1973**, *58*, 985.
(13) (a) McLauchlan, K. A. In *Advanced EPR: Applications in Biology and Biochemistry*; Hoff, A. J., Ed.; Elsevier: New York, 1990; pp 354–369. (b) Trifunac, A. D.; Lawler, R. G.; Bartels, D. M.; Thurnauer, M. C. *Prog. React. Kinet.* **1988**, *14*, 43.
(14) Koptyug, I.; Turro, N. J., private communication.
(15) Forbes, M. D. E.; Ruberu, S. R. *J. Phys. Chem.* **1993**, *97*, 13223.
(16) (a) Encinas, M. V.; Funabashi, K.; Scaiano, J. C. *Macromolecules* **1979**, *12*, 1167. (b) Salvin, R.; Meybeck, J.; Faure, J. *Makromol. Chem.* **1977**, *178*, 2275. (c) Kilp, T.; Guillet, J. E. *Macromolecules* **1981**, *14*, 1680. (d) Scaiano, J. C.; Lissi, E. A.; Stewart, L. C. *J. Am. Chem. Soc.* **1984**, *106*, 1539.
(17) Silverstein, R. M.; Bassler, B. A.; Morrill, T. C. *Spectrometric Identification of Organic Compounds*, 5th ed.; Wiley: New York, 1991, pp 300 and 301.
(18) Lewis, F. D.; Johnson, R. W.; Ruden, R. A. *J. Am. Chem. Soc.* **1972**, *94*, 4292.
(19) (a) Closs, G. L.; Forbes, M. D. E. *J. Phys. Chem.* **1991**, *95*, 1924. (b) Closs, G. L.; Forbes, M. D. E.; Piotrowiak, P. *J. Chem. Soc.* **1992**, *114*, 3285.
(20) (a) Gloux, J.; Guglielmi, M.; Lemaire, H. *Mol. Phys.* **1970**, *19*, 833. (b) Marx, R.; Bonazzola, L. *Mol. Phys.* **1970**, *19*, 899. (c) Kawamura, T.; Koyama, T.; Yonezawa, T. *J. Am. Chem. Soc.* **1973**, *95*, 3220. (d) Kawamura, T.; Koyama, T.; Yonezawa, T. *J. Am. Chem. Soc.* **1970**, *92*, 7222.
(21) (a) Brumbaugh, J. S.; Whittle, R. R.; Parvez, M.; Sen, A. *Organometallics* **1990**, *9*, 1735. (b) Ozawa, F.; Hayashi, T.; Koide, H.; Yamamoto, A. *J. Chem. Soc., Chem. Commun.* **1991**, 1469.